Three-Dimensional Inelastic Stress Analysis of Center Notched Composite Laminates with Damage

C. L. CHOW* AND FAN YANG
Department of Mechanical Engineering
University of Michigan-Dearborn
Dearborn, MI 48128-1491

ABSTRACT: In this paper, a constitutive model for characterization of mechanical response in inelastic composite materials due to damage developed recently by the authors is first outlined. The formulation is based on the concept of damage surface and on the assumption that the change of material behavior is independent of loading path over which the damage state of material develops, but is dependent on the current stress state and the energy dissipated. The method is applied to describe the behaviors of graphite fiber reinforced composite laminates containing a small hole. The elastic-damaged response of interlaminar stresses in the composite laminates due to uniaxial tension is investigated with the aid of displacement-based finite element method. The initiation and development of damage zones in the laminates are examined using a three-dimensional analysis. The results of interlaminar stress distributions of the composite laminates analyzed with and without taking material stiffness degradation into account under the same external loading condition are presented and discussed.

INTRODUCTION

MOST LAMINATED STRUCTURES of engineering importance made of fibrous composites require a three-dimensional analysis even under in-plane loading conditions. The out-of-plane stresses, e.g., interlaminar shear and normal stress components, are important in analyzing the behavior of laminates. For practical reasons, there is an increasing interest in assessing the response of laminates with curved free edges. For example, functional reasons require the presence of through-thickness cut-outs which may be circular, square, or of some other shapes in various composite components. These cut-outs are geometric discontinuities and will result in stress concentrations which could become a source of failure. For instance, the tensile interlaminar normal stresses or interlaminar

*Author to whom correspondence should be addressed.

1056-7895/97/01 23-28 $10.00/0

shear stresses can lead to delamination failures at relatively low applied load levels, because the interlaminar strength is usually low in a laminated structure. Thus, to couple these stress concentrations with the three-dimensional and steep variation behavior of stresses near free edges at the hole boundary is of critical importance in determining the integrity of composite structures. Numerous investigations have been performed in an attempt to study the problem with different methods of analysis, such as, boundary layer theory [1], finite element method [2–5], hybrid stress models [6,7], finite difference theory [8], perturbation approach [9], and stress potential function solution [10]. Most of these methods, however, were limited to the composite material with linear elastic properties. The three-dimensional inelastic characteristics of a composite structure have not been fully treated due to the complexity of the problem.

It is well established that some internal microstructural changes of a material, such as nucleation and growth of distributed microscopic cavities and cracks will not only induce macro-cracks, but will also lead to deterioration of the material properties (e.g., strength, rigidity, and fracture toughness) and decrease remaining lifetime. This phenomenon of progressive degradation of a material prior to initiation of a macro-crack is referred to as damage. Past investigations have revealed that the complexity of material damage in fiber reinforced composite laminates renders an exact analytical solution describing the fine details of a particular damage event untenable. Fortunately, internal damage in composite laminates is noncatastrophic. It is rational to consider locally averaged effect of damage due to micro-cracks/voids in a material element as an equivalent continuous and homogeneous element which can be characterized with a set of internal state variables. Based on the thermodynamics of irreversible process, the internal state variables chosen are used to model the material damage state and the evolution equations for progressive material damage. This approach is usually referred to as the internal state variable approach of damage mechanics. Recently, Allix et al. [11], Kamimura [12], Talreja [13], and Allen and Lee [14] presented several damage models for composite laminates. In their models, damage entities were represented by an appropriate set of average vector- or tensor-valued internal state variables with which the constitutive relations for elastic composite containing distributed damage was formulated. Although these studies offered a way to incorporate the micromechanics level damage mechanisms into macromechanics failure modes, their attention was focused on the prediction of stiffness loss of the laminate for a certain damage state. More recently, Chang et al. [15] conducted a damage analysis of laminated composite containing an open hole. The analysis is based on a two-dimensional laminated theory, thus neglecting the effect of delamination. In addition, the parameter chosen to depict defect geometry is arbitrary without justification. As proper understanding and knowledge of damaging process and its effect on the macroscopic behavior of composite materials are important for the assessment of integrity in practical engineering

structures, a damage mechanics model has been developed by Chow and Yang [16,17] for analyzing nonlinear response of composite laminates with damage.

The purpose of this study is to examine the damage effect on interlaminar stress distributions near a circular hole boundary of composite laminates subjected to a uniformly loaded uniaxial tension remote from the hole. The material model proposed by Chow and Yang [16,17] is first introduced briefly as its application will be extended in the investigation. A three-dimensional displacement-based finite element program is developed for the present analysis because of its versatility in handling the circumstances with nonhomogeneous and nonlinear material properties, irregular specimen shapes, complex boundary conditions, and general loading conditions. The computed damage stress and pseudo-elastic stress for the graphite/epoxy $[0/90°]_s$ and $[90/0°]_s$ laminates are presented and discussed. The damage stress defined in the paper takes into account the progressive stiffness degradation, whereas the pseudo-elastic stress refers to the stress without stiffness degradation. The initiation and growth of damage zones, and the specific form of the failure modes of these laminates are also investigated. The investigations reveal that the stress distributions in the composite laminates containing a through-thickness circular hole are significantly affected by the inclusion of inelasticity generated by the damage of constituent plies.

CONSTITUTIVE RELATION FOR COMPOSITE LAMINA WITH DAMAGE

As current attention is concentrated on the inelastic behavior of composite lamina with damage, a damage model first proposed by Chow and Yang [16] was later extended by the authors [17], where the deviation from the elastic response of the composite ply during loading is considered as a result of the nucleation of new damage entities and the growth of existing damage entities. The model reveals that if an ideal material element is deformed with increasing damage, and then unloaded, it will recover elastically. During unloading, the effective elastic modulus, determined from the initial slope of an unloading curve, remains constant. Furthermore, damage of the material element will not progress unless its initial unloading state is surpassed when reloaded. This problem can be solved by constructing a damage surface in stress space, which also represents initial and subsequent damage surfaces in that space. This damage surface may be expressed as:

$$F(\sigma_i, D) = 0 \tag{1}$$

which is the damage function defined to describe the state of stress σ_i ($i = 1, 2, \ldots, 6$, and the contracted notation and summation convention are adopted) and the internal variable D. D is a measure of damaged deformation and hence

changes only when damage progresses. F is assumed to be continuously differentiable with respect to its arguments. When the stress state is within F, the behavior of the material is elastic; if the stress point reaches the boundary F, i.e., if $F = 0$, a subsequent increment of stress may either cause purely elastic deformation or lead to damage process depending on the direction of the increment. The elastic region is defined as the loci of stress paths along which the damage state of material element does not change.

If time, rate, and environmental effects such as temperature and moisture are excluded and strain is small, the reversible strain components ϵ_i^r of composite lamina in a fixed damage state can be expresssed through the following stress and strain relation:

$$\epsilon_i^r = C_{ij}\sigma_j \quad \text{or} \quad \sigma_i = S_{ij}\epsilon_i^r \quad \text{(for fixed } D\text{)} \tag{2}$$

in which C_{ij} ($C_{ij} = C_{ji}$) and S_{ij} ($S_{ij} = S_{ji}$) are the current material elastic compliance and stiffness, respectively, and $[S_{ij}]^{-1} = [C_{ij}]$, if the inverse exists.

In a damaging process, from Equation (2), the total strain increment can be linearly decomposed into elastic and damaged portions:

$$d\epsilon_i^r = C_{ij}d\sigma_j + dC_{ij}\sigma_j = d\epsilon_i^e + d\epsilon_i^d \tag{3}$$

where the superscripts e and d refer to the elastic and damaged strain components, respectively. Thus, one has

$$d\epsilon_i^e = C_{ij}d\sigma_j \quad \text{and} \quad d\epsilon_i^d = dC_{ij}\sigma_j \tag{4}$$

The incremental damaged strain may also be evaluated based on the damage function F,

$$d\epsilon_i^d = d\lambda\frac{\partial F}{\partial \sigma_i},\ d\lambda > 0, \quad \text{when } F = 0 \text{ and } \frac{\partial F}{\partial \sigma_i}d\sigma_i > 0 \tag{5}$$

where $d\lambda$ is a scalar of proportionality and can be determined from the consistency condition $dF = 0$. This consistency condition implies that the stress state σ_i always lies on the boundary of surface F during a damaging process.

Here, the energy per unit volume dissipated is selected as damage variable and its increment can be written as

$$2dD = \sigma_i d\epsilon_i^d \tag{6}$$

From Equations (3) and (4), one has

$$d\sigma_i = S_{ij}(d\epsilon_j^r - d\epsilon_j^d) \tag{7}$$

and after determining the damaged strain increment from Equations (5), (6), and (1) as well as the consistency condition, the relationship between the elastic-damaged stress increments and the reversible strain increments can be finally expressed as [17]:

$$d\sigma_j = S_{ij}^{ed} d\epsilon_j^r \tag{8}$$

where

$$S_{ij}^{ed} = S_{ij} - \frac{S_{ik}\dfrac{\partial F}{\partial \sigma_k}\dfrac{\partial F}{\partial \sigma_l}S_{lj}}{\dfrac{\partial F}{\partial \sigma_m}S_{mn}\dfrac{\partial F}{\partial \sigma_n} - \dfrac{1}{2}\dfrac{\partial F}{\partial D}\sigma_p\dfrac{\partial F}{\partial \sigma_p}} \tag{9}$$

which is the elastic-damaged instantaneous tangent modulus matrix. It should be emphasized that the values of S_{ij}^{ed} in this equation are not constants. Usually, S_{ij}^{ed} is a function of stress state and is dependent upon the previous loading histories that involve damage progression. Equations (2) and (8) provide a general constitutive description for an elastic-damaged composite material.

The damage surface shown in Equation (1) may be taken as:

$$F(\sigma_i, D) = (R_{mn}\sigma_m\sigma_n)^{1/2} - K(D) = 0 \tag{10}$$

where the coefficients R_{ij} ($R_{ij} = R_{ji}$ is assumed) depict the influence of each stress component on the material damage state and can be determined from experiments, and $K(D)$ is a state function and changes when D develops. Furthermore, the equivalent stress σ_o and the equivalent damaged strain increment $d\epsilon^d$ are defined as:

$$\sigma_o^2 = R_{mn}\sigma_m\sigma_n \quad \text{and} \quad 2dD = \sigma_i d\epsilon_i^d = \sigma_o d\epsilon^d \tag{11}$$

and $\sigma_o - \epsilon^d$ relation established from the experiment is:

$$\epsilon^d = \langle m\sigma_o^n - m\sigma_s^n \rangle \tag{12}$$

where m and n are positive constants, σ_s is the equivalent stress at the threshold of damage, and the $\langle\rangle$ symbol is a function defined as:

$$\langle x \rangle = \begin{cases} x, \text{ if } x > 0 \\ 0, \text{ if } x \leq 0 \end{cases}$$

With the postulation that damage effects are relected through the variation of material elasticity and the material coefficients C_{ij} are merely a function of damage state D, independent of the damaging processes [18], the following equations can be derived from Equations (4), (5), (10), (11), and (12):

$$C_{ij}(D) = C_{ij}(0) + \frac{mn}{(n-1)}\langle \sigma_o^{n-1} - \sigma_s^{n-1} \rangle R_{ij} \tag{13}$$

and

$$D = \frac{mn}{2(n+1)}\langle \sigma_o^{n+1} - \sigma_s^{n+1} \rangle \quad (\text{for } d\sigma_o \geq 0) \tag{14}$$

where C_{ij} (0) denotes the compliance of the lamina without damage. From Equation (13), it can be seen that the coefficients R_{ij} reflect the anisotropic behavior induced by material damage. During a damaging process, Equation (13) is employed to predict instantaneous C_{ij} values. For unloading, the coefficients C_{ij} remain constant and are determined from σ_o at the start of unloading. Upon reloading, D as well as C_{ij}, do not change unless σ_o exceeds its previous maximum value. Given the constitutive description of composite lamina, the response of composite laminate under loading can be analyzed since the composite ply is taken as a building block of composite laminate.

FORMULATION OF THE PROBLEM

The laminate considered here is a rectangular plate subjected to uniaxial in-plane loading symmetric about the midplane. The construction of the laminate is also symmetric about its midplane so that there is no extension/bending coupling of the plate due to the external load. A composite laminate of total thickness $t = 2H$ is made of $2m$ layers of composite lamina of thickness h (i.e., $2H = 2mh$), with overall width $2b$ and length $2a$. The laminate has a central circular hole of radius of R. The ratio of laminate thickness to hole diameter is about 0.25. To analyze this problem, the rectangular and cylindrical coordinate systems X, Y, Z and r, ϕ, Z are introduced. The origin of both coordinate systems is fixed at the center of the hole on the midplane of the laminate, $Z = 0$, see Figure 1. The laminate is stretched by a uniform extension ϵ_0 along X axis at the specimen ends far away from the hole. Both the top and the bottom surfaces of the laminate as well as the edge of the hole are free of traction.

For the sake of illustration, two types of lamination, $[0/90°]_s$ and $[90/0°]_s$, of graphite/epoxy composite laminates, i.e., $m = 2$ are chosen. The fiber direction of 0° layer coincides with the loading direction, while the fiber direction of 90° ply is perpendicular to the loading direction. A three-dimensional finite element

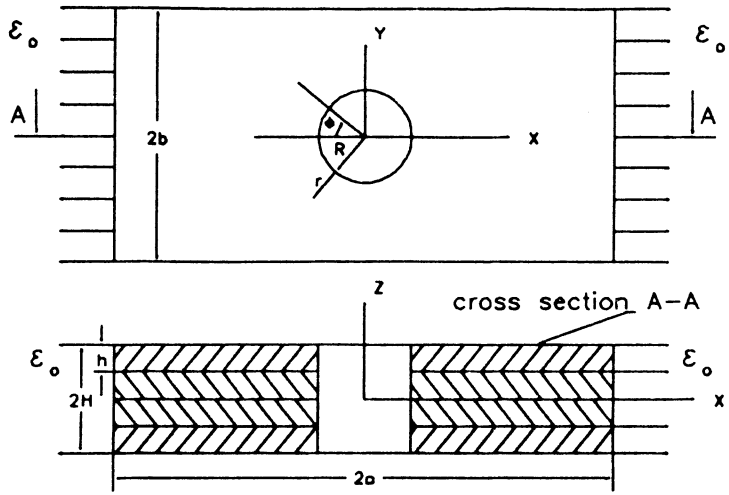

Figure 1. *Composite laminate containing a hole subjected to uniaxial extension.*

procedure of elastic-damaged analysis of fibrous composite structures based on the proposed model will be utilized. The numerical procedure is similar to that of the conventional nonlinear analysis. The main difference lies in the stress-strain relations, which currently include damage effects, and the modification of the stiffness matrix during calculation is necessary. A modified Newton-Raphson method with Aitken acceleration scheme, owing to its computational efficiency, is employed to solve the corresponding finite element equations. In the stress analysis, through specifying appropriate displacement boundary conditions, only one-eighth of the whole laminate bounded by $-a \leq X \leq 0$, $0 \leq Y \leq b$, and $0 \leq Z \leq H$ due to the symmetrical configurations and loading condition is considered and it is discretized by three-dimensional 20-node isoparametric volume elements. The element represents a unidirectional composite lamina with fibers arbitrarily orientated in the laminate coordinates. Laminated structures with layers in several directions are built up by joining individual unidirectional elements. In the finite element analysis, each lamina may be represented with at least one element in the thickness direction. Obviously, one element cannot be used to represent two or more consecutive laminae as their material axes may not coincide. Thus, it is possible that the finite element discretization may contain elements of the type which have one dimension much smaller than the other two dimensions. Care must therefore be exercised to construct the finite element mesh for which the largest and smallest dimensions of an element do not differ by more than one order of magnitude. Otherwise, numerical ill-conditioning of the element's stiffness matrix may result.

A typical finite element mesh pattern that is used in analyzing the problems for two constituent laminae in the laminate is depicted in Figure 2. In order to account for the steep stress gradients, the mesh is comparatively refined at close proximity of the through-thickness hole boundary. Each constituent ply is represented by three sublayers in which each sublayer consists of thirty-six elements and each ply therefore contains 108 elements. Different thickness values of the sublayers along the Z direction are used in order to more accurately describe the stress variations near the interface between 0 and 90 degree layers, see Figure 2.

In the finite element stress analysis, laminate layers are modeled as three-dimensional homogeneous and orthotropic materials suffering elastic-damaged behaviors. Individual fibers and matrix are not considered. This yields valuable informaiton and is computationally efficient. With the finite element discretization of the proposed composite nonlinear damage model, the stress distribution as well as the damage behavior of composite laminates containing a central circular hole can be readily solved.

From Reference [16], the initial undamaged material properties of the composite lamina made of 648 epoxy matrix reinforced with sixty-five volume percent of T300 graphite fibers are

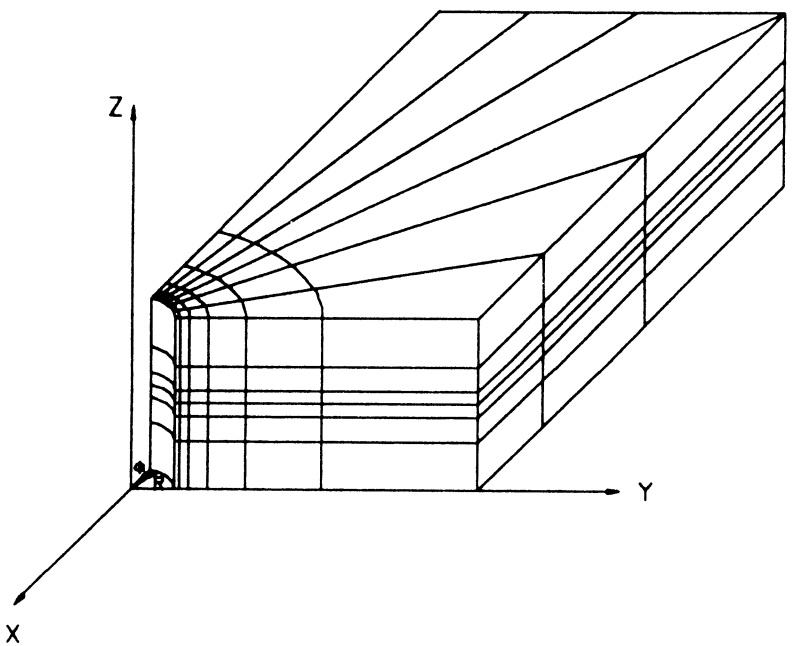

Figure 2. *Finite element model for the laminate with a hole.*

$$E_{11} = 1.25 \times 10^5 \text{ MPa}, E_{22} = E_{33} = 1.11 \times 10^4 \text{ MPa}, \nu_{23} = 0.338$$

$$\nu_{21} = \nu_{31} = 0.03, G_{12} = G_{13} = G_{23} = 3.3 \times 10^3 \text{ MPa}$$

The relevant material coefficients in Equations (11) and (12) for the composite lamina with damage determined from a series of uniaxial tensile tests of the unidirectional composite laminates with different orientations are

$$m = 0.114 \times 10^{-4}, n = 1.242, \sigma_s = 9.0 \text{ MPa}$$

and the R_{ij} values which do not vanish are

$$R_{22} = R_{33} = 1, R_{44} = R_{55} = R_{66} = 1.9, \text{ and } R_{23} = 0.05$$

These material coefficients will be used as the input data for the finite element analysis.

RESULTS AND DISCUSSIONS

For the $[0/90°]_s$ laminate, it is of interest to note that damage starts at the point $Z/2h = 0.715$, $\phi = 71.82°$ on the hole boundary of the 0° layer at the external extension $\epsilon_0 = 154.34\mu\epsilon$. This is due to a higher level of combined normal and shear stresses at that location. Damage initiation at the perimeter of the hole in 90° layer is found at a higher applied extension level. The results of the individual stress component σ_{xx}, σ_{yy}, σ_{xy}, σ_{zz}, σ_{xz}, and σ_{yz} distributed in 90° and 0° laminae around the curved free edge of the hole in the $[0/90°]_s$ laminate at the applied extension ϵ_0 of $154.34\mu\epsilon$ are shown in Figures 3–8, respectively. To illustrate the three-dimensional effect, stress distributions at different Z distances are also presented. In the 90° lamina, all the predictions reveal that no significant stress concentrations are found at $\phi = 90°$. The circumferential stress concentration σ_{xx} near the midplane at the location $\phi = 90°$ in the 0° lamina is about eleven times that in the 90° lamina. In contrast, the corresponding stress σ_{yy} at the location $\phi = 0°$ in the 90° layer is about thirteen times that in the 0° ply. In-plane shear stress σ_{xy} is maximum at $\phi = 71.82°$ at the top surface of the 0° layer of the laminate. Although the strains vary continuously across the thickness Z, the in-plane stress components are discontinuous across the 0/90° interface because of the different fiber orientations of the two adjacent layers. It is worth pointing out that the maximum normal stress σ_{zz} takes place at the angle of $\phi = 33.2°$ which is along the midplane of the laminate. The out-of-plane shear stress components are much more significant along the 0/90° interface plane, in which the highest value of stress σ_{xz} and σ_{yz} occurs at the angle of 63.18° and 48.18°, respectively. Actually, the interlaminar shear stress components are the

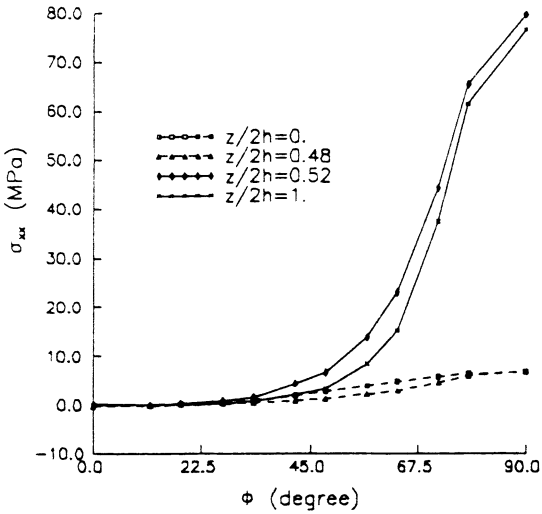

Figure 3. *σ_{xx} distributions around the hole in $[0/90°]_s$ laminate.*

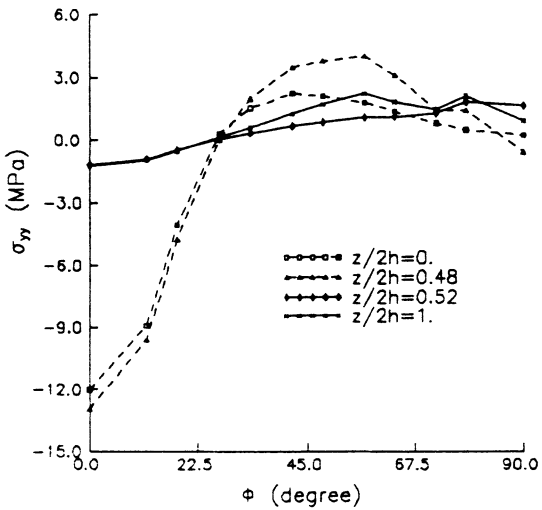

Figure 4. *σ_{yy} distributions around the hole in $[0/90°]_s$ laminate.*

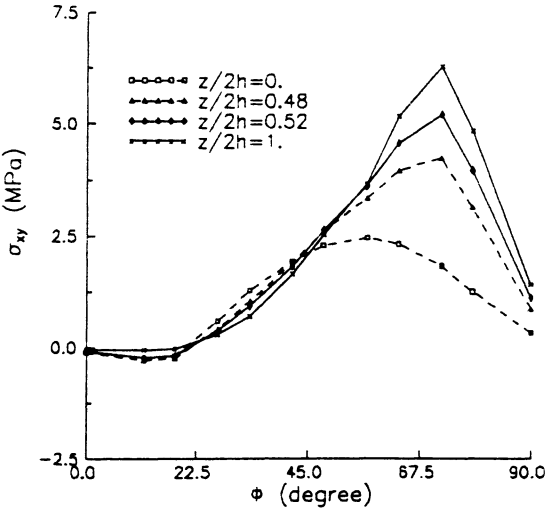

Figure 5. *σ_{xy} distributions around the hole in $[0/90°]_s$ laminate.*

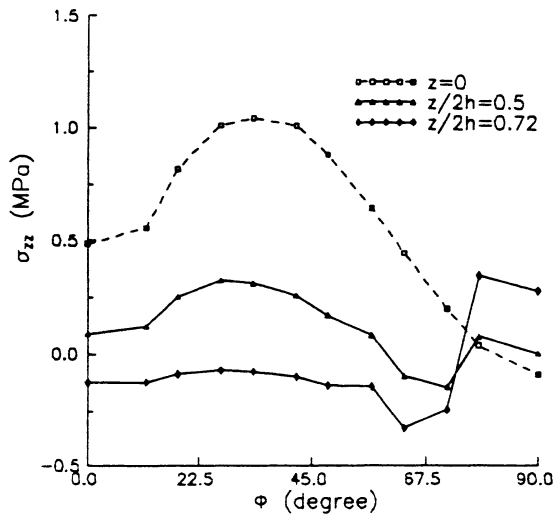

Figure 6. *σ_{zz} distributions around the hole in $[0/90°]_s$ laminate.*

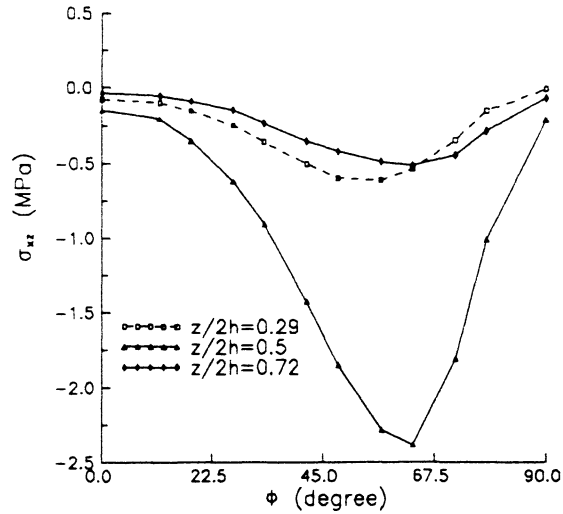

Figure 7. *σ_{xz} distributions around the hole in $[0/90°]_s$ laminate.*

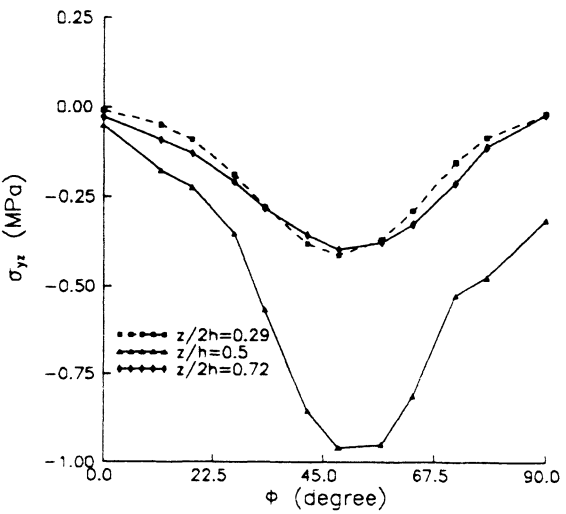

Figure 8. *σ_{yz} distributions around the hole in $[0/90°]_s$ laminate.*

direct products of mismatch between the in-plane material behaviors at the free edge. They should be zero at $\phi = 0°$ and $\phi = 90°$ as expected because there is no in-plane shear stress at these two locations. However, away from these two locations, the in-plane shear stresses result from the curvilinear boundary of the hole, and consequently, interlaminar shear stresses grow rapidly. Investigation on the stress distributions provides a better understanding of the damage initiation and development in the laminate. Figure 9 shows some damage contours on the hole boundary surface of the $[0/90°]_s$ laminate. At lower strain level, it can be seen that damage develops mainly along the hole boundary. As the applied strain increases, more and more material points at the hole edge start to experience damage.

In the case of $[90/0°]_s$ laminate, the variations of individual stress components within the laminate along the curved free edges of the hole across different Z levels are illustrated in Figures 10–15 for external extension strain $\epsilon_0 = 151.42\mu\epsilon$. Similar results to those obtained in the $[0/90°]_s$ laminate can be observed. Comparing with the $[0/90°]_s$ laminate, the difference between the two laminates can be easily identified. For both laminates, the in-plane stress components have very similar distributions in the corresponding laminae, while the out-of-plane stress components in the two laminates are of opposite sign.

Damage in the $[90/0°]_s$ laminate is first observed in the material element of the hole surface at $\phi = 71.82°$ near the midplane of the laminate, i.e., on the edge of the bottom surface of the 0° layer, when $\epsilon_0 = 151.42\mu\epsilon$. Also plotted in Figure 16 are several damage contours on the hole edge of the laminate at different applied strain levels. Similar conclusions on the damage development can be drawn

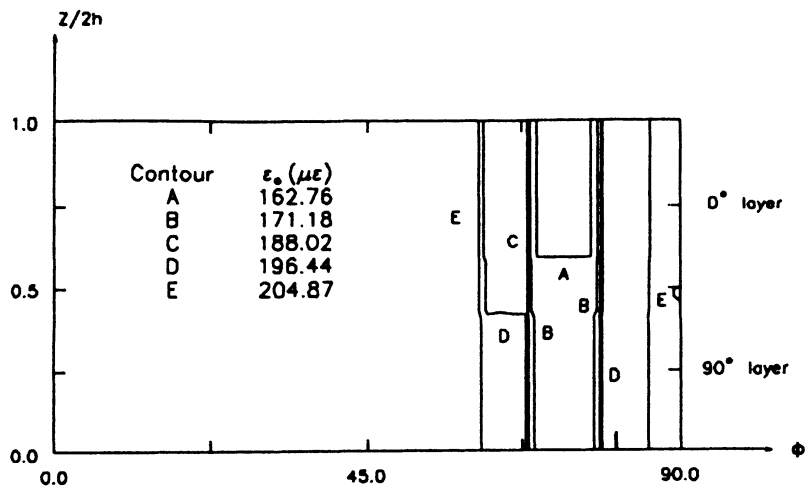

Figure 9. *Damage contours on the hole surface in* $[0/90°]_s$ *laminate.*

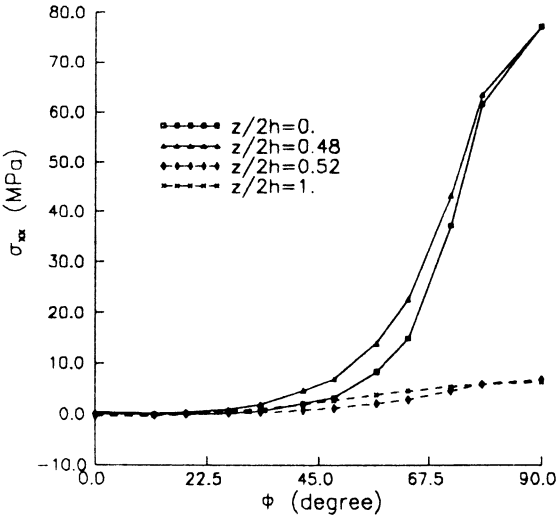

Figure 10. *σ_{xx} distributions around the hole in $[90/0°]_s$ laminate.*

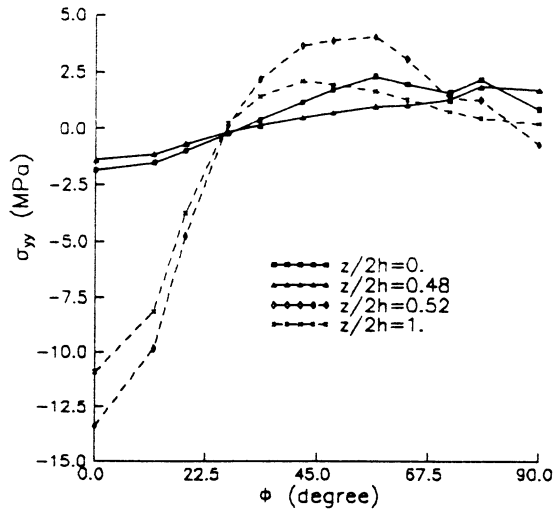

Figure 11. *σ_{yy} distributions around the hole in $[90/0°]_s$ laminate.*

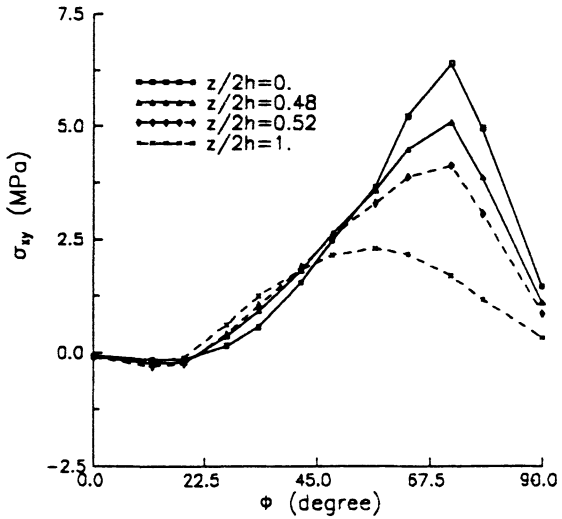

Figure 12. *σ_{xy} distributions around the hole in $[90/0°]_s$ laminate.*

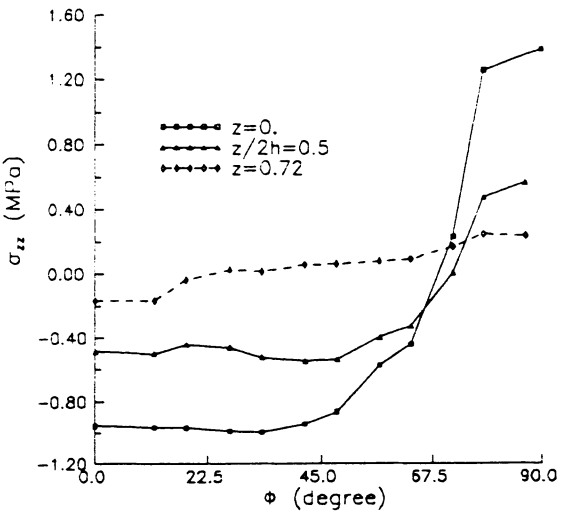

Figure 13. *σ_{zz} distributions around the hole in $[90/0°]_s$ laminate.*

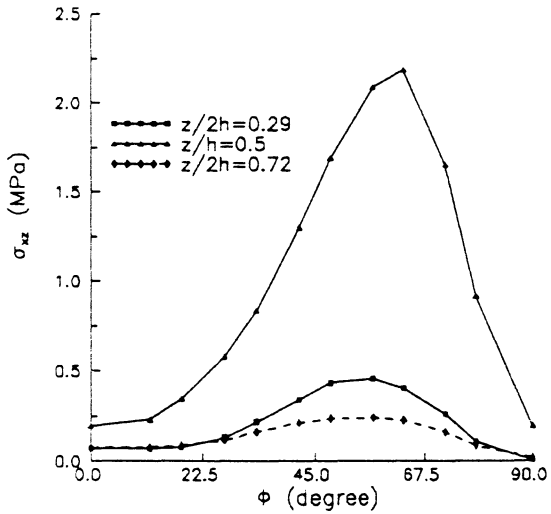

Figure 14. *σ_{xz} distributions around the hole in $[90/0°]_s$ laminate.*

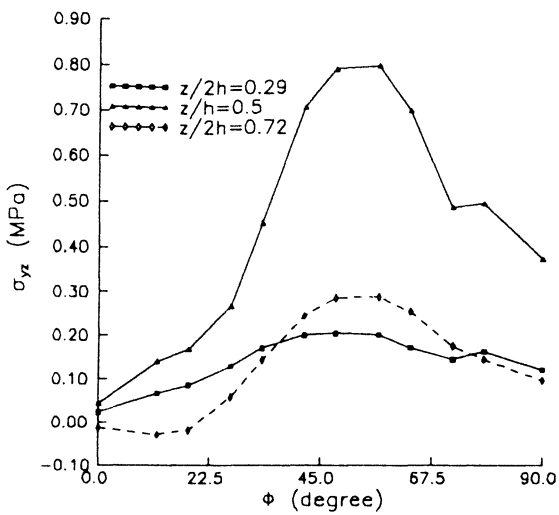

Figure 15. *σ_{yz} distributions around the hole in $[90/0°]_s$ laminate.*

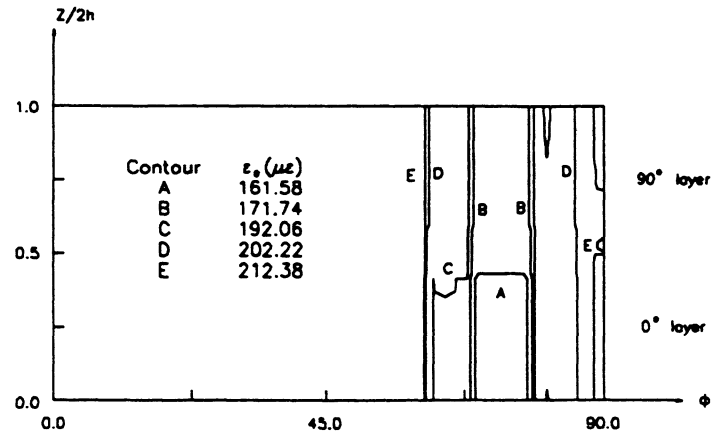

Figure 16. *Damage contours of the hole surface in* $[90/0°]_s$ *laminate.*

for the laminate as that of $[0/90°]_s$ laminate. Comparing the two laminates, one may also conclude that the threshold condition of damage initiation in the $[90/0°]_s$ laminate is marginally lower than that in the $[0/90°]_s$ one.

The damage zones within each layer of the $[0/90°]_s$ laminate at different applied strain levels are illustrated in Figure 17 and Figure 18, respectively. To demonstrate the three-dimensional behaviors, the damage development on the top and bottom surfaces of each layer is also presented. Several general conclusions can be drawn from the examinations of the plots. Obviously, the shape and evolution of the damage zones within each layer of the laminate are different. When the ap-

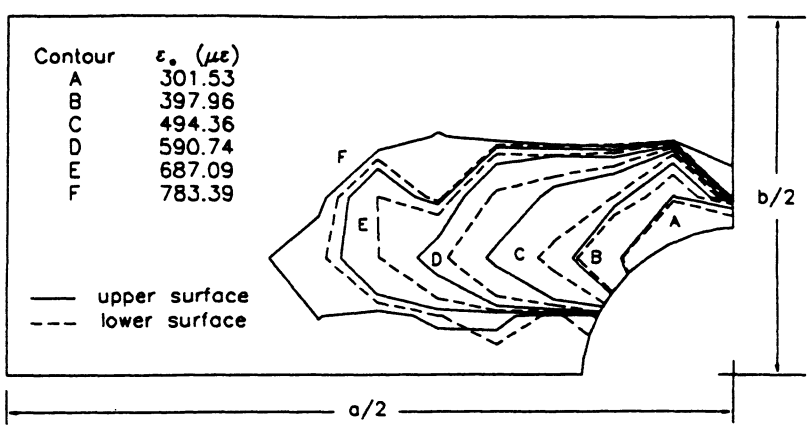

Figure 17. *Damage contours in the 0° layer of* $[0/90°]_s$ *laminate.*

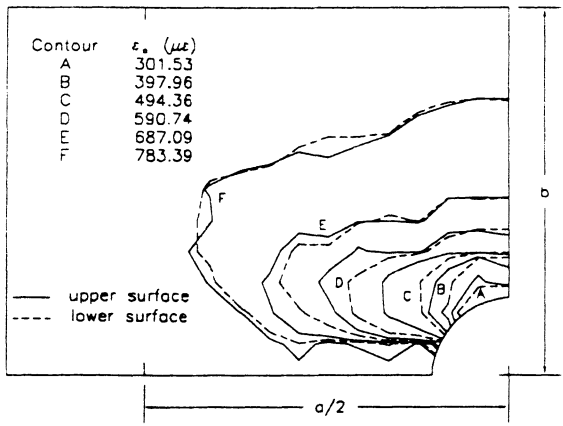

Figure 18. *Damage contours in the 90° layer of* $[0/90°]_s$ *laminate.*

plied strain level is lower, the damage zone remains localized and expands outward from the hole boundary with increase in load. The 90° ply has a larger damage zone which tends to grow across the width of the specimen, while the damage zone in the 0° layer is narrow and extends along the length of the specimen. The net section damage is, as expected, prevalent in the 90° lamina at a certain remotely applied strain level, whereas the damage zone in the 0° ply remains constrained to the vicinity of the hole. This distinctive response may be attributed to the presence of $R_{1j} = 0$ ($j = 1, 2, \ldots, 6$) which manifests a strong damage anisotropic behavior caused by the stiff graphite fibers in the layer. In other words, the larger the magnitude of the combined shear and transverse stresses is developed, the larger would be the size of the damage zone in each ply along the direction of the combined stresses. Similar observation can also be made for the damage development in the $[90/0°]_s$ laminate as shown in Figure 19 and Figure 20.

In order to illustrate the damage influence on the stress repsonse of the laminates containing a central hole, the distribution of individual stress component along the direction of $\phi = 33.2°$ will be examined in detail. This angle is chosen because the damage development appears to be in general much pronounced along this particular direction. Similar study may be readily made for other ϕ directions.

The variations of the in-plane normal stress components σ_{xx} and σ_{yy} of the $[0/90°]_s$ laminate in the $\phi = 33.2°$ direction with the normalized radial coordinate r/R, when the applied uniaxial extension strain $\epsilon_0 = 783.4\mu\epsilon$, are shown in Figure 21 and Figure 22, respectively. The results on top and bottom surfaces in each layer are also displayed to illustrate the through-thickness effect. To demonstrate the damage effect on stress distributions, the pseudo-elastic results evaluated based on the virgin laminate stiffness without damage are also included.

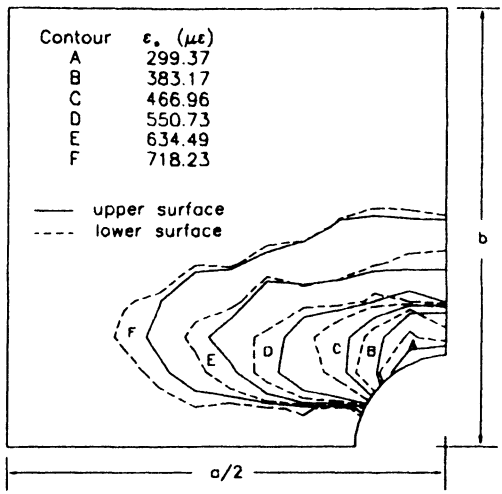

Figure 19. *Damage contours in the 90° layer of* $[90/0°]_s$ *laminate.*

From Figure 21a, it can be seen that the damage influence on stress σ_{xx} in 0° layer is not evident due to this stress component parallel to the direction of fibers. As the radius increases, the stress value reaches a stable level. This indicates the highly localized influence of the hole. However, in the 90° ply, the σ_{xx} is perpendicular to the fiber direction and its value changes due to damage development, as depicted in Figure 21b. At the prescribed strain level, the pseudo-elastic stress σ_{xx} at the 0/90° interface near the hole boundary is about 8.47 MPa in the 0° layer

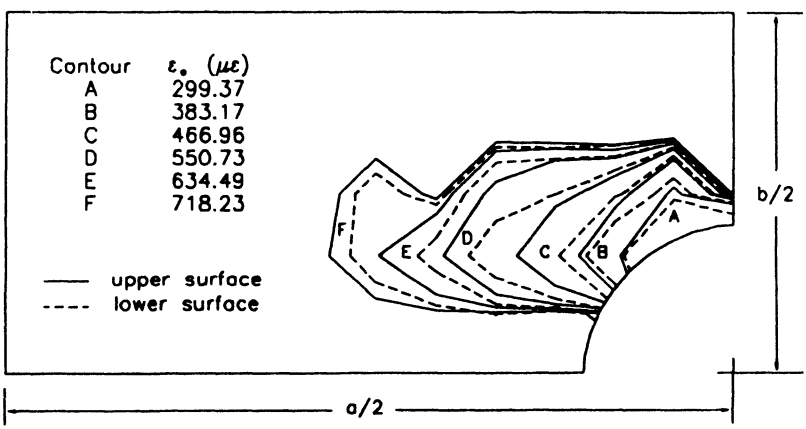

Figure 20. *Damage contours in the 0° ply of* $[90/0°]_s$ *laminate.*

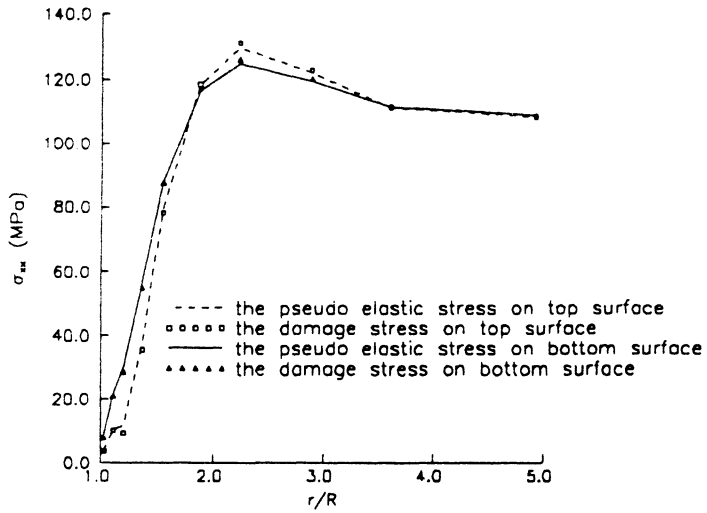

Figure 21a. *σ_{xx} distributions in the 0° layer of $[0/90°]_s$ laminate.*

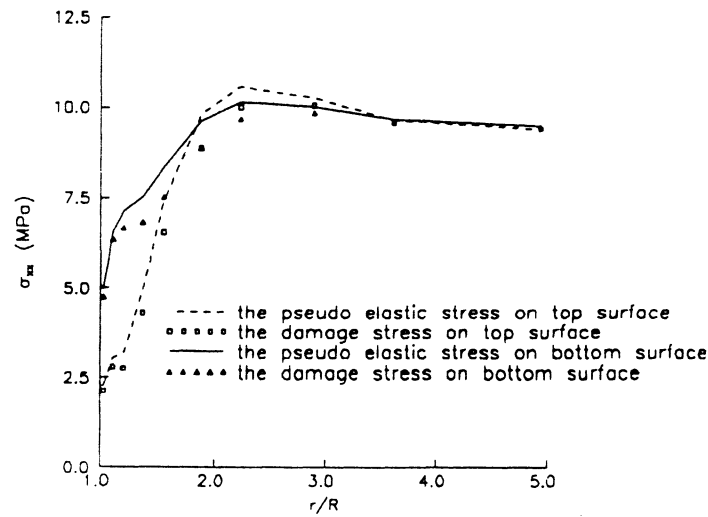

Figure 21b. *σ_{xx} distributions in the 90° layer of $[0/90°]_s$ laminate.*

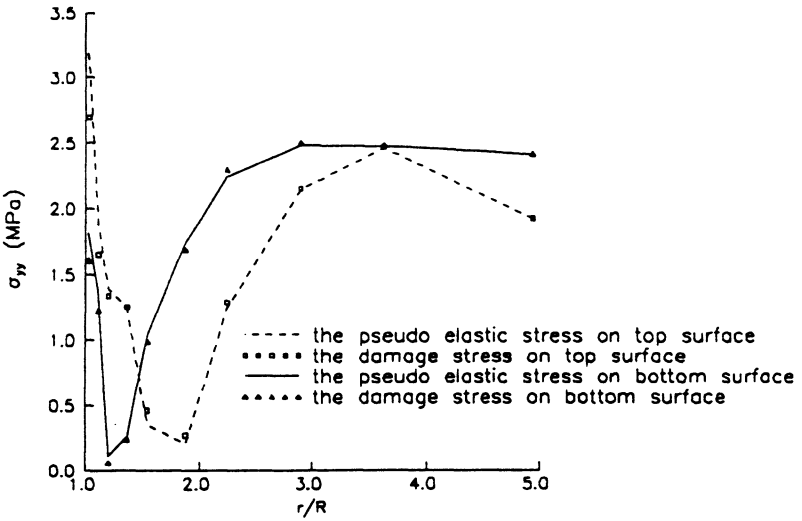

Figure 22a. *σ_{yy} distributions in the 0° layer of $[0/90°]_s$ laminate.*

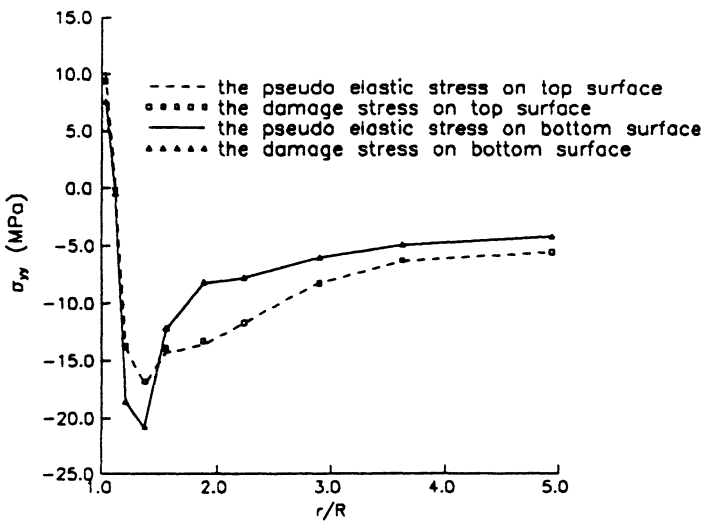

Figure 22b. *σ_{yy} distributions in the 90° layer of $[0/90°]_s$ laminate.*

and 2.28 MPa in the 90° ply. If the inelasticity due to damage is taken into account, the material deterioration effect could result in a lower σ_{xx} in the constituent lamina. For instance, at the same position on the 0/90° interface, the value of damage stress σ_{xx} predicted by the proposed damage model is reduced to about 2.14 MPa in the 90° layer, while in the 0° layer it is about 7.86 MPa. It should be pointed out that the damage effect on σ_{xx} is not as significant on the top surface of the 90° ply as on the bottom surface because of the reinforcing effect of the 0° fibers in the upper layer. In Figure 22a, a noticeable damage effect on stress σ_{yy} within the 0° ply can also be observed. It is more pronounced on the top surface than on the bottom surface of the layer in which the damage development is constrained by the reinforced fibers of the subsequent 90° lamina. The σ_{yy} distribution in 90° ply determined by the damage theory is not very different from that by linear elasticity as this stress component coincides with the fiber direction of the layer. However, its maximum value is reudced, as shown in Figure 22b. The typical tensile stress exists in the 0° layer, but a compressive stress is present in the 90° ply and it changes abruptly from tension to compression near the hole edge. The in-plane shear stress component σ_{xy} distributions in the laminate calculated with and without taking stiffness degradation into account are plotted in Figure 23. Damage effect generally causes a decrease in stress magnitude due to stress redistribution. The rapidly diminishing property of the stress confirms that, far away from the hole, the in-plane shear stress will vanish.

Under the applied uniaxial extension $\epsilon_0 = 783.4\mu\epsilon$, the variation of the interlaminar transverse normal stress σ_{zz} at the 0/90° interface and the midplane of

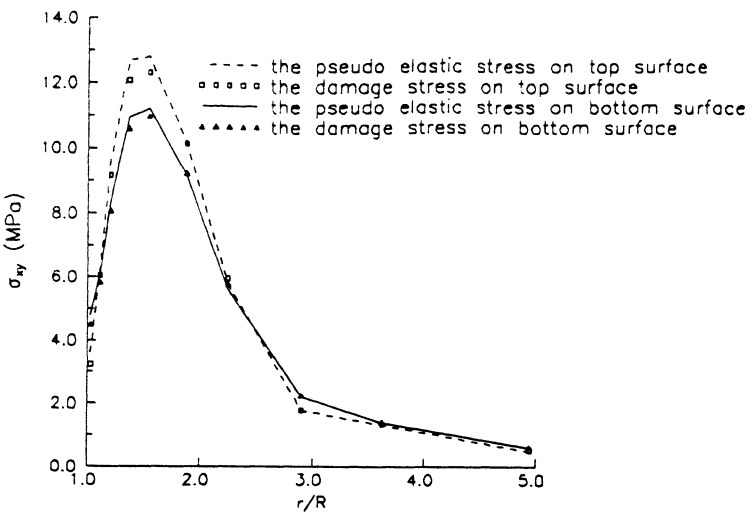

Figure 23a. *σ_{xy} distributions in the 0° layer of $[0/90°]_s$ laminate.*

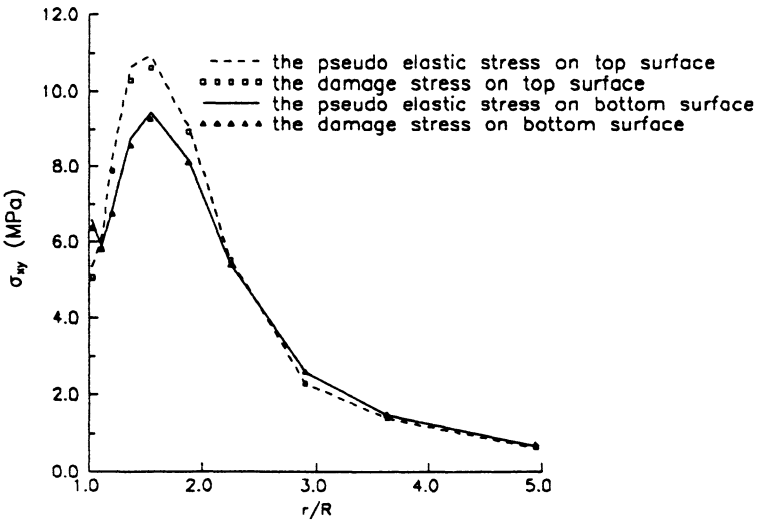

Figure 23b. *σ_{xy} distributions in the 90° layer of $[0/90°]_s$ laminate.*

the $[0/90°]_s$ laminate along the $\phi = 33.2°$ direction with the radial coordinate r/R is illustrated in Figure 24. A higher magnitude of the stress is shown along the midplane than along the interface of the laminate. The σ_{zz} is mainly tensile and is much larger near the hole edge. It diminishes rapidly from the edge of the hole. As the raduis increases, the damage effect decreases. The distributions of interlaminar shear stresses σ_{xz} and σ_{yz} with the normalized radial coordinate r/R along the 0/90° interface of the $[0/90°]_s$ laminate for $\epsilon_0 = 783.4\mu\epsilon$ are shown in Figure 25 and Figure 26, respectively. For the prescribed tensile strain, insignificant differences can be observed between the damaged and the corresponding pseudo-elastic stress distributions. However, the peak levels of these stress components near the hole edge in the inelastic case are lower than those of the pseudo-elastic stress. For instance, the maximum value of pseudo-elastic σ_{yz} is about -2.9 MPa, while the maximum damage stress is about -2.8 MPa. Examination of the hole circumference near the interface reveals that at the given tensile strain value, the interlaminar shear and normal stresses tend to approach zero rapidly from the hole edge. As the σ_{zz} and σ_{yz} magnitudes are comparatively small, among the interlaminar stress components, σ_{xz} is thus more likely the dominant stress for the delamination initiation at the curved free edge. It is of interest to note that the maximum value of σ_{xx} is not located at the hole edge like those of σ_{zz} and σ_{yz}, but at the location close to the hole edge, see Figure 25. The diminishing nature of these interlaminar stress distributions also indicates that they can be neglected in the areas far away from the hole.

Similar distributions in terms of σ_{xz}, σ_{zz}, and σ_{yz} for $[90/0°]_s$ laminate,

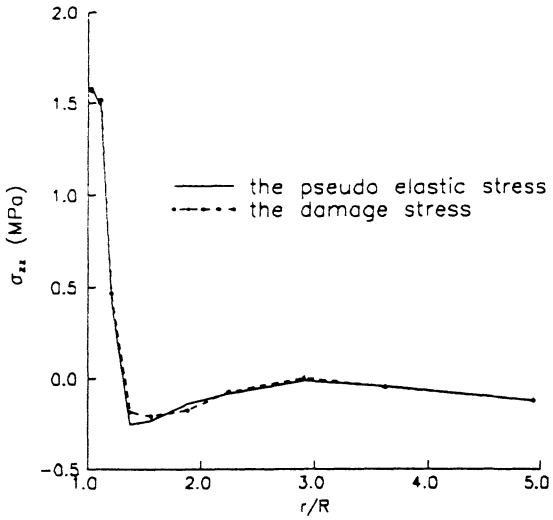

Figure 24a. *σ_{zz} distributions along 0/90° interface of $[0/90°]_s$ laminate.*

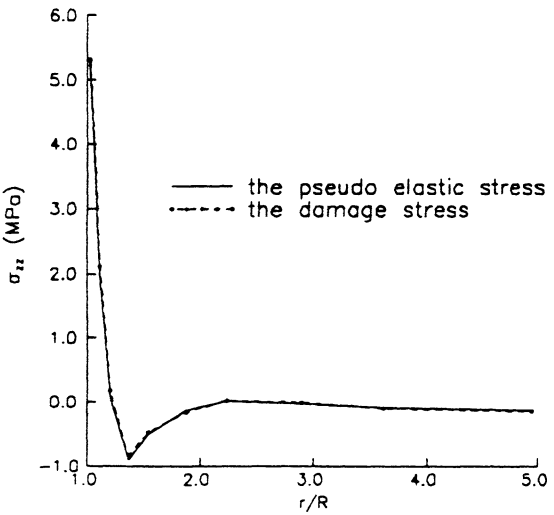

Figure 24b. *σ_{zz} distributions along midplane of $[0/90°]_s$ laminate.*

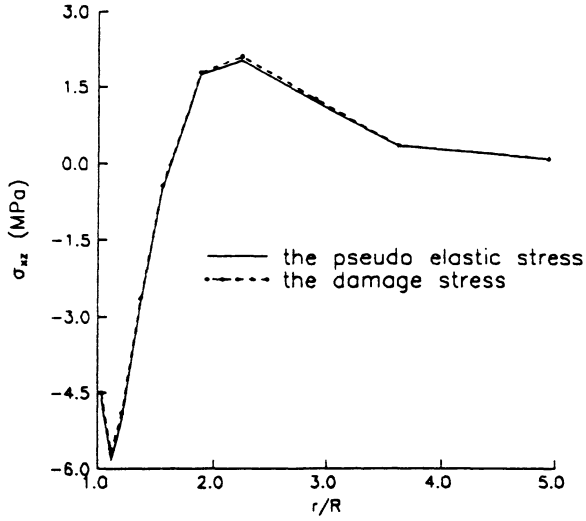

Figure 25. *σ_{xz} distributions along 0/90 interface of $[0/90°]_s$ laminate.*

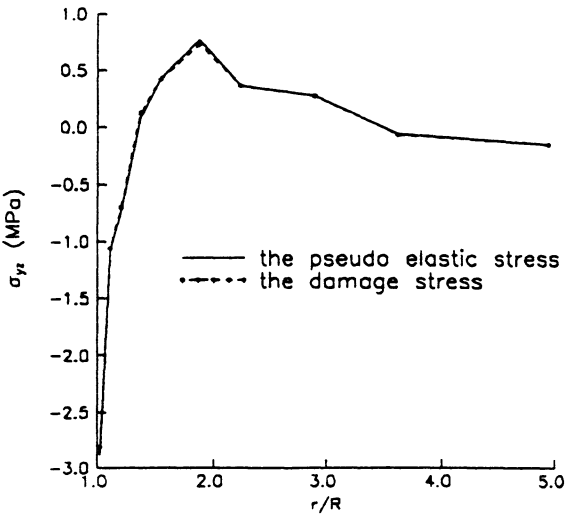

Figure 26. *σ_{yz} distributions along 0/90 interface of $[0/90°]_s$ laminate.*

calculated with the damaged stiffness and the non-damage coupled material coefficients are also investigated. Compared with those in the $[0/90°]_s$ laminate, it is worth noting that change in the stacking sequence does not significantly influence the distributions of in-plane stress components in corresponding lamina, but the signs of interface and midplane interlaminar stresses are reversed. Similar conclusions on the damage effect of stress distributions to those in $[0/90°]_s$ laminate can also be drawn.

CONCLUSIONS

In this study, a three-dimensional elastic-damaged stress analysis of fiber reinforced composite laminates containing a circular hole, with the aid of the developed finite element program, has been presented. Based on the analysis of the characteristics of the laminate, the failure mode, damage zone, and its progress, can be quantified. According to the description of damage in composite lamina, the stiffness matrix of those elements in the damage zone can be modified, and then new stress distributions result. This stress redistribution determines the subsequent development of damage zone and the load capacity of the laminates, which would not otherwise be possible using the conventional non-damage coupled stress analysis.

The numerical results computed show that high interlaminar stress gradients occur at the through-thickness hole boundary and the interlaminar stress distributions around the circular hole have different characteristics from those of the straight boundary. The damage analysis of composite laminates containing a circular hole subjected to a uniaxial remote extension loading also demonstrates the distinct three-dimensional behavior of damage zone development within each layer. Investigation of the graphite/epoxy $[0/90°]_s$ and $[90/0°]_s$ laminates illustrates the significant effects of material anisotropy on initiation and progression of damage as well as the induced interlaminar stress redistribution. It is anticipated that better accuracy of prediction on the response of composite laminates may be obtained if the interaction of damage characteristics among its constituent plies is considered.

The numerical calculations presented herein also indicate that a three-dimensional displacement-based finite element procedure can be used successfully to predict progressive failure process in notched composite laminates in terms of the initiation and propagation of damage zones. More accurate numerical results could be obtained if more refined finite element models are used. In addition, this work can be further applied to analyze more complex structures, for example, a laminate containing curvilinear holes under arbitrary loading conditions. Other effects such as hole size, layer thickness, stacking sequence, and different notch forms on stress distributions and damage development in the composite laminates can also be investigated.

It is clear that damage can cause a very complex influence on the response of

laminated composite structures. But with the aid of a numerical tool such as the proposed finite element procedure, the analyst is now equipped with the capacity to conveniently and effectively quantify this intriguing material and structural behavior. Based upon the available results on the interlaminar stresses in composite laminates, it is understood that such interlaminar stresses only occur in the immediate neighborhood of the free edge. Therefore, for the investigation of interlaminar stresses in a composite laminate containing a circular through-thickness hole, instead of considering the entire laminate as a three-dimensional body, a simplified model may be adopted in such a way that only the immediate area to the circular hole is treated as a three-dimensional problem while the remaining region is considered an anisotropic plate. Such a substructuring model can significantly reduce the amount of computational work and still provide valuable information for engineering design purposes.

Of principal concern in the description of composite structures is the prediction of their ultimate failure loads. It is possible to extend the proposed analysis scheme to include progressive failure study of notched composite laminates if a proper fracture criteria is incorporated for the constituent unidirectional laminae. However, a very large computer storage space and lengthy computational work are required to solve this problem.

This paper presents a three-dimensional finite element analysis for a notched composite plate. A separate study is in progress to measure strain distributions in a similar notched plate. Initial results agree well with those reported in the paper and the study will be presented in a later publication.

REFERENCES

1. Tang, S. 1977. "Interlaminar Stresses around Circular Cutouts in Composite Plates under Tension," *AIAA J.*, 15:1631–1637.
2. Rybicki, E. F. and D. W. Schmueser. 1978. "Effect of Stacking Sequence and Lay-Up Angle on Free Edge Stresses around a Hole in a Laminated Plate under Tension," *J. of Composite Materials*, 12:300–313.
3. Lee, J. D. 1982. "Three Dimensional Finite Element Analysis of Damage Accumulation in Composite Laminate," *Computers & Structures*, 15:335–350.
4. Carlsson, L. 1983. "Interlaminar Stresses at a Hole in a Composite Member Subjected to In-Plane Loading," *J. of Composite Materials*, 17:238–249.
5. Klang, E. C. and M. W. Hyer. 1985. "Damage Initiation at Curved Free Edges: Application to Uniaxially Loaded Plates Containing Holes and Notches," *Recent Advances in Composites in the United States and Japan, ASTM STP 864*, J. R. Vinson and M. Taya, eds., pp. 62–90.
6. Nishioka, T. and S. N. Atluri. 1982. "Stress Analysis of Holes in Angle-Ply Laminates: An Efficient Assumed Stress 'Special-Hole-Element' Approach and a Simple Estimation Method," *Computers & Structures*, 15:135–147.
7. Chen, W. H. and T. F. Huang. 1989. "Three Dimensional Interlaminar Stress Analysis at Free Edges of Composite Laminate," *Computers & Structures*, 32:1275–1286.
8. Altus, E. and A. Dorogoy. 1989. "A Three-Dimensional Study of Delamination," *Engg. Fract. Mech.*, 33:1–19.

9. Bar-Yoseph, P. and J. Avrashi. 1985. "Interlaminar Stress Analysis for Laminated Plates Containing a Curvilinear Hole," *Computers & Structures,* 21:917-932.
10. Shalev, D. and K. L. Reifsnider. 1989. "Influence of Relative Ply Orientations on the Nature of the Edge Effect Singularities for a Circular Hole in a Composite Laminate," *Int. J. of Solids & Structures,* 25:1115-1132.
11. Allix, O., P. Ladeveze, E. L. Dantec and E. Vittecoq. 1990. "Damage Mechanics for Composite Laminates under Complex Loading," *Yielding, Damage, and Failure of Anisotropic Solids, EGF5,* J. P. Boehler, ed., Mechanical Engineering Publications, London, pp. 551-569.
12. Kamimura, K. 1985. "Continuum Damage Approach to Mechanical Behavior of Damaged Laminate and a Modelling of Damage Parameter," *Mechanical Characterization of Load Bearing Fiber Composite Laminates,* A. H. Cardon and G. Verchery, ed., Elsevier Applied Science Publishers Ltd., pp. 115-126.
13. Talreja, R. 1990. "Internal Variable Damage Mechanics of Composite Materials," *Yielding, Damage, and Failure of Anisotropic Solids, EGF5,* J. P. Boehler, ed., Mechanical Engineering Publications, London, pp. 509-533.
14. Allen, D. H. and J. W. Lee. 1990. "Matrix Cracking in Laminated Composites under Monotonic and Cyclic Loadings," *ASME-AD,* 111:65-75.
15. Chang, F. K., K. Y. Chang and S. Liu. 1991. "Damage Tolerance of Laminated Composites Containing an Open Hole and Subjected to Tensile Loadings," *Journal of Composite Materials,* 25:274-301.
16. Chow, C. L. and F. Yang. 1992. "A Simple Model for Brittle Composite Lamina with Damage," *J. of Reinforced Plastics & Composites,* 11(3):222-242.
17. Chow, C. L., F. Yang and A. Asundi. 1992. "A Method of Nonlinear Damage Analysis for Brittle Materials and Its Application to Thin Composite Laminates," *Int. J. of Damage Mechanics,* 1(3):347-366.
18. Schapery, R. A. 1990. "A Theory of Mechanical Behavior of Elastic Media with Growing Damage and Other Changes in Structure," *J. Mech. Phys. Solids,* 38:215-253.